Photochemistry of Adsorbed Molecules. 19. Photodissociation of CH_3I on LiF(001) and NaCl(001) at 248 nm: REMPI Probing of CH_3

J. C. Polanyi,* N. S.-K. Sze, and J.-X. Wang

Department of Chemistry, University of Toronto, Toronto, Ontario, Canada M5S 3H6

Received: March 17, 1997; In Final Form: May 23, 1997[⊗]

The photodissociation of CH_3I on LiF(001) and NaCl(001) at 248 nm has been studied by probing the CH_3 fragments, using angular-resolved resonantly enhanced multiphoton ionization and time-of-flight mass spectrometry. At submonolayer and multilayer coverages, the translational energy, vibrational state, and angular distributions of the CH_3 photofragments were determined for both CH_3I/LiF and CH_3I/NaCl. The translational-energy distributions for the fast component of the CH_3 fragments resembled those for the gas phase, indicative of collision-free recoil from the substrate. The I* quantum yields obtained from adsorbed CH_3I were, however, substantially lower than for the gas. At multilayer coverage the I* quantum yield from adsorbed CH_3I was found to vary as a function of vibronic band of the CH_3 photofragments, from 0.76 for the 0_0^0 band to 0.34 for the 2_2^2 band. These results were rationalized on the basis of the Landau−Zener model for potential-energy surface hopping. The measured vibrational-state distributions of the umbrella mode also exhibited a strong dependence on reaction channel, on coverage, and on substrate. The angular distributions depended on the substrate; a sharp peak at 20° was observed in the angular distribution for the CH_3I/LiF system, whereas a broader peak characteristic of collisional scattering was obtained for CH_3I/NaCl. These angular distributions indicated that CH_3I(ad) was close to upright on LiF but tilted further away from the normal on NaCl. The energy distributions, which showed evidence of greater collisional deexcitation on NaCl than on LiF, appeared consistent with these differing adlayer geometries.

I. Introduction

The photochemistry of adsorbates has been the focus of many recent studies.[1] The primary interest lies in what has been termed "Surface Aligned Photochemistry" (SAP);[2] the study of the dynamics of photodissociation and photoreaction in aligned and ordered adlayers. Until now, few experiments have been performed with state resolution of the products, though this is an established way to study molecular reaction dynamics in the gas phase.[3]

In the present work, we report for the first time on studies of photodissociation of CH_3I adsorbed on LiF(001) and NaCl(001) surfaces, in which the translational energy, vibrational state, and angular distributions of the CH_3 photofragments have been determined using resonantly enhanced multiphoton ionization (REMPI) technique[4] and time-of-flight mass spectrometry (TOF-MS).

The $\tilde{A}$ band photodissociation of CH_3I in the gas phase has been studied extensively in the past years.[5−11] These experimental investigations have stimulated a large number of theoretical studies.[12] The photodissociation dynamics can be described as follows: The CH_3I is excited to the $^3Q_{0+}(A_1)$ state through a $\sigma^* \leftarrow n$ electronic transition and then directly dissociates into $CH_3 + I$ (or I*) due to the strongly repulsive nature of this state. The atomic iodine is formed primarily in its excited-state $I^*(^2P_{1/2})$, however, a curve crossing with the $^1Q_1(A', A'')$ surface also produces iodine in its ground-state $I(^2P_{3/2})$. Measurement of the I* quantum yield has been the subject of previous studies.[9−11]

The CH_3 radicals are produced with ν_2 "umbrella" mode excitation, since CH_3 goes from a pyramidal to a planar structure during photodissociation. There has been disagreement in the vibrational state distributions reported for the gas phase. The earlier TOF-MS studies[5−7] and infrared emission experiments[8] suggested that CH_3 was highly vibrationally excited, based on the TOF spectra and on measurements of photofragment infrared emission spectra. The vibrational state distributions were reported to peak at $\nu_2 = 2$ for I* channel and $\nu_2 = 4$ for I channel. However, no inverted vibrational-state distributions were observed in recent REMPI experiments[10] and infrared diode laser studies[11] by directly probing the vibrational levels of the CH_3 photofragments. The latter findings represent the current view.

There have been two previous experimental studies of the photodissociation of CH_3I adsorbed on insulator surfaces; those by Welge and co-workers[13] and a series of studies by Stair, Weitz, and co-workers.[14] In the earlier work the Welge group studied the dissociative desorption of thick solid CH_3I on LiF-(001) surface.[13] The yields of both CH_3 and CH_3I were obtained at various laser fluences, using REMPI spectroscopy. It was found that direct dissociation was strong at laser fluences below 1.5 mJ/cm^2, whereas "explosive" desorption dominated at higher laser fluences. Subsequent workers (this group among them) have avoided these higher fluences.

Stair, Weitz, and co-workers studied the photodissociation of CD_3I on MgO(100) at 257 nm, detecting both methyl and iodine fragments using REMPI techniques.[14] Though the internal energy distributions in CD_3 were not obtained, the REMPI spectrum and translational-energy distribution resembled that for the gas phase. The measured I* quantum yield was substantially reduced from that in the gas phase. They postulated that the adsorbed CD_3I molecules on MgO(100) adopted an ordered antiparallel geometry with the C−I bond aligned along the surface normal.

Additionally there has been theoretical modeling of the photodissociation dynamics of CH_3I on LiF(001).[15] Two equilibrium configurations of CH_3I at a given temperature were found by a Monte Carlo simulation; both configurations had the CH_3I molecular axis perpendicular to the surface, but one

[⊗] Abstract published in *Advance ACS Abstracts,* July 15, 1997.

S1089-5639(97)00965-1 CCC: $14.00

had the methyl group up and one down. The dissociation dynamics was followed by means of classical molecular dynamics. The angular distribution, translational energy, and rovibrational state distributions of the CH_3 fragments were calculated. For the case of methyl pointing up, the kinetic energy and internal state distributions were similar to those in the gas phase. When CH_3 pointed down, collisions of CH_3 with the surface and with the iodine photofragment broadened the kinetic energy distribution of the CH_3 and cooled the vibrational distribution in the umbrella mode.

In the present studies of the photodissociation of adsorbed CH_3I, we examine a range of dynamical properties on two substrates, differing in ionic-mesh size; LiF(001) and NaCl-(001). The measurables are translational energy, vibrational energy, and angular distribution. The variables include coverage on each substrate.

We give a detailed description of the experiments in section II. In section III, we report the translational energy, vibrational state, and angular distributions of the CH_3 photofragments. In the same section we discuss the reaction dynamics based on the present and related experimental findings. A brief summary is to be found in section IV.

II. Experiment

The ultrahigh-vacuum (UHV) system used in these experiments has been described in previous publications from this laboratory.[16] It is equipped with several detection systems. Two of them were employed in the present studies: polarized Fourier transform infrared absorption (FTIR) spectrometry, which will be fully described in a separate publication,[17] and a movable TOF−REMPI ion-detection assembly. Typically, after several days of baking at 130 °C, the chamber was at a pressure of $\sim 2 \times 10^{-10}$ Torr when pumped by a combination of turbomolecular pump, oil diffusion pump, and rotary mechanical pump during the experiments.

Both LiF and NaCl crystals (UV grade, Solon Technology Inc., Harshaw Bicron) were cleaved in air and then mounted immediately on the sample holder for pump-down. The sample holder was mounted on top of a vertical copper rod attached to a closed-cycle refrigerated displex (APD Cryogenics Inc.). The whole assembly could be translated and rotated by means of an *xyz* manipulator and a rotary platform.

After chamber bakeout, the sample was continuously heated at ∼450 K for at least 24 h for annealing. This procedure was repeated after each cycle of experiments. The cleanness of the samples was examined by comparing our FTIR spectra for CH_3F/LiF and CO_2/NaCl with published spectra[18,19] and also by directly probing the LiF(001) surface using X-ray photoelectron spectroscopy (XPS) in a separate setup in this laboratory.[20] These tests showed that the sample treatment described above was sufficient to obtain and maintain a clean crystal surface ($\ll$5% contamination).

A typical "pump−probe" laser system was employed in these experiments. The photolysis (pump) laser was a Lumonics excimer (TE−861T-4) at 248 nm, used to dissociate CH_3I adsorbed on the surfaces. It was unpolarized. The fluence was ≤ 1.0 mJ/cm^2 for multilayer coverage and 4−10 mJ/cm^2 for submonolayer coverage. The analysis (probe) laser was produced by frequency doubling (Inrad, Autotracker II) of the output of a tunable dye-laser (Quanta-Ray, PDL-1) which was pumped by a Nd:YAG laser (Quanta-Ray, DCR-2). The spectral range was from 320 to 335 nm for probing CH_3 photofragments using the REMPI technique. The output was typically 1−3 mJ/pulse. The lasers were operated at 10 Hz for all the experiments reported here.

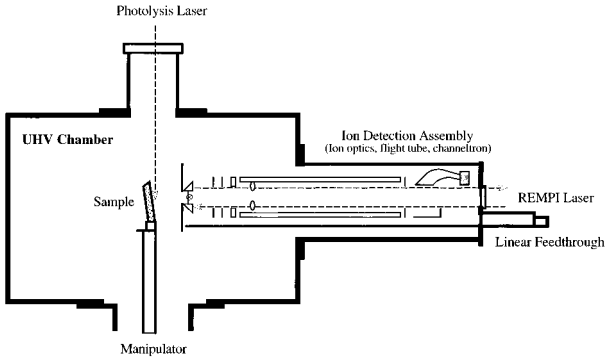

Figure 1. Schematic diagram of the UHV chamber and the ion detection assembly. (The plane of the focused and reflected REMPI laser beam has been shown rotated through 90° from its actual geometry.)

A schematic diagram of the chamber and the TOF ion detection assembly is shown in Figure 1. The detection assembly consisted of a repeller plate, a set of ion optics, a 20 cm flight tube, and a channeltron electron multiplier. There were also two pairs of prism/lens assemblies in the chamber to guide and focus the analysis beam. The optical system used to focus the REMPI laser beam has been described previously.[16] The whole detection assembly was mounted on a linear-motion feedthrough so that the flight distance to the focal point could be adjusted from approximately 3.4 to 6.7 cm.

The photolysis laser entered the chamber through a top window along the axis of the manipulator and irradiated the crystal surface which was tilted by 10° with respect to the incoming laser beam. The center of the sample was aligned to face the axis of the flight tube. The analysis laser entered and exited the chamber through two small windows at the end of the ion detection assembly. It passed in front of the sample surface, parallel to it, at a distance that was adjustable by way of the linear motion described above. The REMPI beam was focused along the axis of the flight tube by means of a fixed focus lens (*f*/5 cm) also inside the chamber. The position of the focal point is indicated by ⊗ in Figure 1.

Methyl iodide (CH_3I, Fisher Chemical 99.9%, BDH 99%) was dosed continuously onto the cold crystal surfaces without further purification through a leak value using a Granville-Phillips 216 pressure/flow controller. The temperature of the crystals was kept at 80 ± 1 K for all experiments. The dosing pressure was kept constant during each experiment in the range from 1.0×10^{-8} to 2.0×10^{-7} Torr, depending on the coverage being studied. The experiments were performed under adsorption/desorption equilibrium conditions which ensured data were collected at almost constant coverages.

The equilibrium conditions were achieved by carefully controlling the photolysis laser power and dosing pressure. In the case of submonolayer coverages, higher laser-power and lower dosing pressure were used so that no CH_3I could accumulate on the substrate between laser pulses. The "submonolayer" coverage used in this work was <0.1 ML. Experiments have been carried out at various coverages within this low coverage. For multilayer coverages a combination of lower laser power and higher dosing pressure was used to obtain various equilibrium coverages in the range 30−50 ML. These coverages were measured by FTIR for multilayer coverages. For submonolayer we determined the coverage by examining the integrated CH_3 ion signal dependence on dosing time, dosing pressure and laser power under the experimental conditions of (photolysis) laser irradiation.

The CH_3 photofragments produced from photodissociation of CH_3I(ad) at 248 nm were detected using the (2+1) REMPI

technique[4] combined with TOF spectrometry. Three modes of operation were used to study the energy partitioning and angular distribution of the CH_3 fragments. For the study of translational energy distribution, TOF spectra were recorded by scanning the time delay between the photolysis and REMPI lasers at a fixed flight distance for a given vibronic transition. The time delay was typically scanned at intervals of $\sim$0.1 μs. For the study of vibrational-state distributions, the REMPI spectra were collected by scanning the analysis laser wavelength at a fixed flight distance and a given laser time delay. The laser scanning step was 0.015 nm. In each case, every data point on the spectra was an average of 20−30 laser pulses. For the study of angular distribution, integrated signal intensity was recorded at each detection (polar) angle using a step interval of 5°, by rotating the sample with respect to surface normal for given vibronic transition, fight distance, and laser time delay. Each data point consisted of an average of 600 laser pulses.

The laser time delay was controlled by a digital delay/pulse generator (Stanford Research, DG535). The signals were collected using a boxcar integrator/averager (Stanford Research, SR250) and a standard computer interface (SR245) on a shot-to-shot basis in the cases of the TOF and REMPI spectra, or a 400 MHz digital oscilloscope (LeCroy 9310A) in the case of the angular distribution. The resulting data were then transferred to a microcomputer (Mac SE/30) through a GPIB interface, for display, storage and analysis. All the results presented here were averaged over a number of measurements.

III. Results and Discussion

(A) Translational Energy Distribution. The translational energy distributions of the methyl photofragments generated from photodissociation of CH_3I on LiF(001) and NaCl(001) were studied using TOF spectroscopy, monitoring the CH_3 ion signal intensity, $P(t)$, as function of flight time, t, at a *known* flight distance, d, from the crystal. The initial flight distance was calibrated by recording a series of TOF spectra at various distances. For each TOF spectrum in the series, the distance was steadily increased by an interval registered on the linear-motion feedthrough of the ion-detection assembly. The resulting plot extrapolated back to zero time at zero distance.

The TOF spectra obtained were converted into translational energy distributions, $P(E_T)$, by multiplying by t^3, since $P(E_T) \propto P(t)t^3$ according to the Jacobian transformation. The translational energy, E_T, could be calculated using d and t since $E_T = {}^1/_2 m(d/t)^2$, where m is the mass of CH_3. As mentioned in section II, the CH_3 fragments were state-selectively ionized using the REMPI technique to select vibrational bands, so that TOF spectra for individual vibronic bands could be obtained.

Figure 2 shows the state-selected translational energy distributions of the CH_3 fragments for the CH_3I/LiF and CH_3I/NaCl systems at both submonolayer and multilayer coverages. All the spectra were taken at a detection angle of 10° from the surface normal. The broad energy distributions ($E_T < 0.6$ eV) corresponding to the slow CH_3 fragments are not shown in these spectra since our primary interest is in the fast CH_3(g) photofragments that can clearly be identified with the photodissociative event. Slower methyl radicals may include those from the photodissociation of intact CH_3I(g) arriving in the REMPI laser-irradiation zone.

The "explosive desorption" described by Welge and coworkers[13] would not be expected to evidence itself in our TOF spectra. "Explosive desorption" requires high laser fluence (>1.5 mJ/cm^2) and multilayer coverage. In our case lower laser fluence ($\leq$1.0 mJ/cm^2) was used for multilayer coverages. Furthermore, "explosive desorption" gives rise to only CH_3 with low translational energy ($E_T \ll 0.5$ eV), whereas this work deals with translational energies $E_T > 0.5$ eV (see Figure 2).

Two distinct peaks were observed in each translational-energy spectrum. These were attributed to the two reaction channels; I* + CH_3 and I + CH_3, termed the I* and I channels. The maximum translational energies for the I* and I channels obtained from the energy spectra of the CH_3I/LiF system (see Figure 2) were approximately 1.7 and 2.4 eV, respectively. These values are in agreement with those reported for direct photodissociation of thick layers of CH_3I/LiF at 248 nm[13] and also with those from theoretical calculations performed for this system for the case that the CH_3 is pointing up.[15] These values are very close to the expected maximum translational energies of 1.5 eV for the I* channel and 2.4 eV for the I channel, from photodissociation of CH_3I in the gas phase at 248 nm *when the internal energy of CH_3 fragments is neglected*.[21] This correspondence is good evidence that the fastest CH_3 fragments observed in our experiments on LiF are produced from photodissociation of CH_3I(ad) to yield CH_3(g) that escapes *directly* from the surface, i.e., the CH_3I must be oriented with the CH_3 up and aligned approximately along the surface normal (see also section III.C).

The observed energy difference between the I and I* peaks is $\sim$0.7 eV, smaller than the spin−orbit splitting of the iodine atom, which is 0.94 eV.[22] A similar value to this experimental one, namely, 0.75 eV, has been obtained by theoretical calculation for CH_3I/LiF system.[15] The discrepancy with E(I*) − E(I) could be due to the fact that the I channel deposits a greater fraction of available energy in CH_3 internal excitation. This is what will be shown to be the case in the present experimental study. The explanation accords with the fact that a spin−orbit splitting energy of 0.95 eV, very close to the value for atomic iodine, was obtained from the TOF spectra of the H atoms from photodissociation of HI/LiF at 193 nm in experiments performed in this laboratory.[23] In the case of HI there is no possibility for a differing fraction of the available energy to be channeled into internal excitation in the I* and I channels.

Comparing the spectra for the CH_3I/NaCl system with those for the CH_3I/LiF system, it is evident that the two peaks for CH_3I/NaCl are broader and shifted to lower energy. This suggests that the geometry of the CH_3I adlayer on NaCl is more of the "lying-down" variety, permitting some of the CH_3 to have a weak collision with neighboring CH_3I(ad) as they leave the surface.[24] The effect on the angular distribution (see section III.C) for CH_3I/NaCl as compared with CH_3I/LiF is in accord with this explanation (the angular distribution is much broader for CH_3 from CH_3I/NaCl than from CH_3I/LiF).

For a given substrate, LiF or NaCl, the effect of increased coverage was a shift of the peak translational energy for the I* and the I channel by roughly 0.1−0.2 eV to higher translational energies and a concurrent narrowing of the peak at fwhm (compare for example the solid lines in Figure 2a with 2b). Both these changes suggest that CH_3I(ad) is more sharply aligned at multilayer coverage. For the case of CH_3I/LiF, which gave a narrower $P(\theta)$ at higher coverage, this improved alignment was evident in the CH_3 angular distribution (see section III.C).

(B) Vibrational-State Distribution. The vibrational-state distributions of the CH_3 photofragments were studied using (2+1) REMPI spectroscopy, monitoring the CH_3 ion signal intensity as function of laser wavelength. Figure 3 shows the REMPI spectra of the CH_3 fragments recorded for CH_3I/LiF and CH_3I/NaCl systems at both submonolayer and multilayer coverages. These spectra were taken at a detection angle of 10° from the surface normal. For a given reaction channel, I* or I, the spectra were obtained by setting the laser time delay

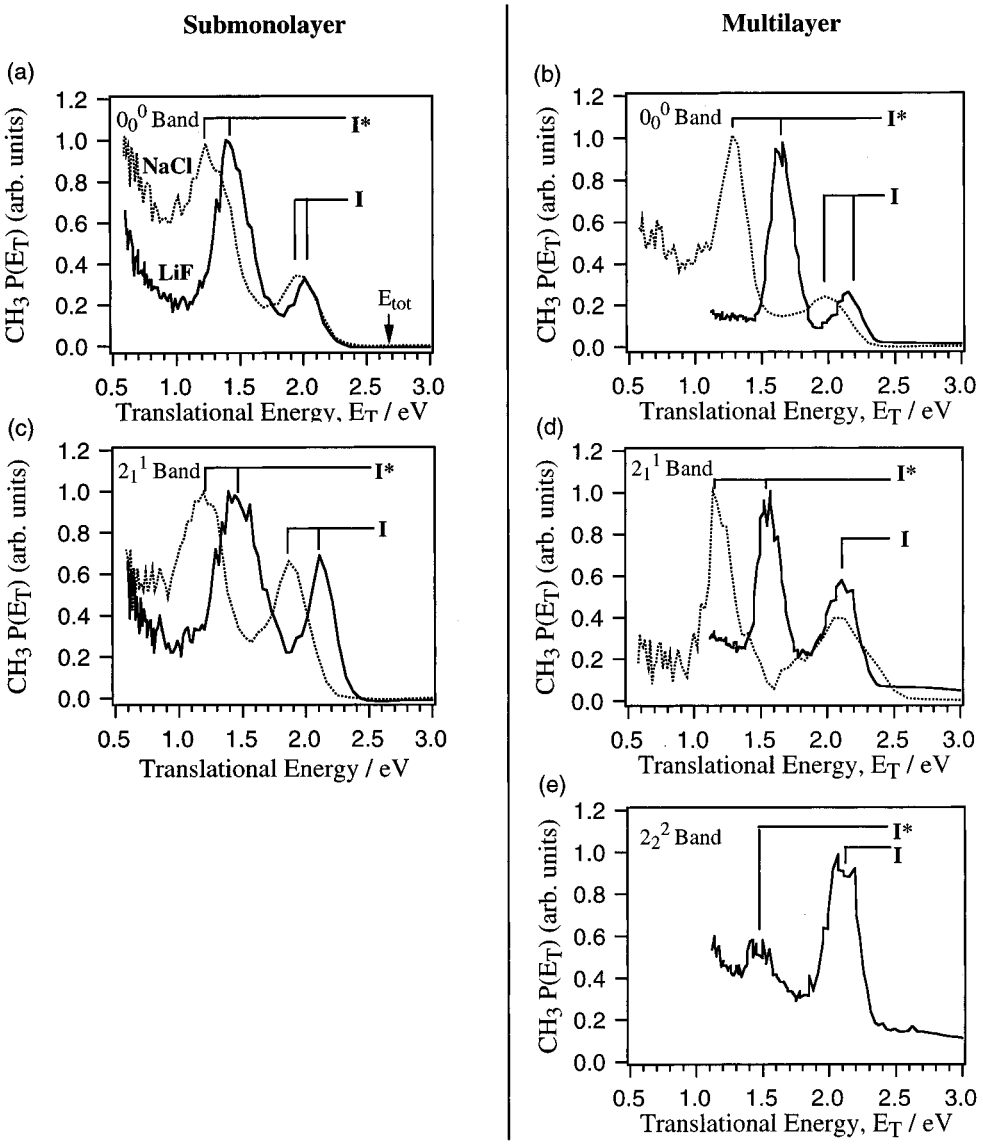

Figure 2. State-selected translational energy distributions of the CH_3 photofragments from photodissociation of CH_3I adsorbed on LiF(001) and NaCl(001) at submonolayer (left column) and multilayer (right column) coverages. The arrow labeled E_{tot} indicates the total available energy for the reaction. Spectra are normalized to their peak values. Solid lines are for the LiF substrate, and dashed lines for NaCl. Measurements were made at an angle of $\theta = 10°$ to the surface normal.

at the corresponding peak positions in the TOF spectra (see section III.A and Figure 2). All the REMPI spectra of Figure 3 have been normalized for variation in photolysis laser power, which was recorded on a shot-to-shot basis together with the ion signal. The photolysis laser power was kept constant, so far as possible, during recording of these spectra.

Three vibronic bands, 0_0^0, 2_1^1, and 2_2^2, were observed in this spectral region. This progression corresponds to the ν_2 out-of-plane bending motion of CH_3, the so-called "umbrella-mode" vibration. The vibrational excitations of $\nu_2 = 2$ (the 2_2^2 band) are visible in Figure 3 in most of the spectra, especially for the I channel. An effort was made to resolve the rotational structures of the strong 0_0^0 and 2_1^1 bands; this failed due to insufficient resolution of the REMPI laser used in the study.

The vibrational-state distributions, $P(\nu_2)$ were obtained from Figure 3 using integrated peak intensities of the vibronic bands and divided by their respective Franck−Condon factors as calculated by Houston and co-workers.[10] It is known that the intermediate state of the CH_3 radical predissociates and that the rate of the predissociation depends strongly on the vibrational levels of that state.[25] Predissociation is found to be more severe for higher vibrational levels; e.g., 70% more predissociation in going from $\nu_2 = 0$ to $\nu_2 = 2$, as determined using 2_2^0 and 2_2^2 bands.[10] This complicates the evaluation of vibrational populations from the REMPI spectra of CH_3. The predissociation effect has not been taken into account in our calculations of the vibrational-state distributions since our main purpose is to assess the effect of substrate, coverage, and reaction pathway on the vibrational population. Such a comparison will not be affected by the predissociation of CH_3 from the intermediate state in the course of REMPI.

Figure 4 shows the vibrational-state distributions obtained from our experiments. Among the cases presented here, the methyl radicals are most excited for the I channel of CH_3I/LiF system at submonolayer coverage (bottom-left pictures in Figures 3 and 4), and least excited for the I* channel of CH_3I/NaCl system at multilayer coverage (top-right pictures in Figures 3 and 4).

The vibrational-state distribution for the I channel of the CH_3I/LiF system at submonolayer coverage obtained here is close to that calculated by Huang and Guo,[15] in which a slight population inversion for $\nu_2 = 1$ was observed when the CH_3 moiety was pointing up. If the population of the $\nu_2 = 2$ level observed here is corrected for the predissociation effect (70% greater for

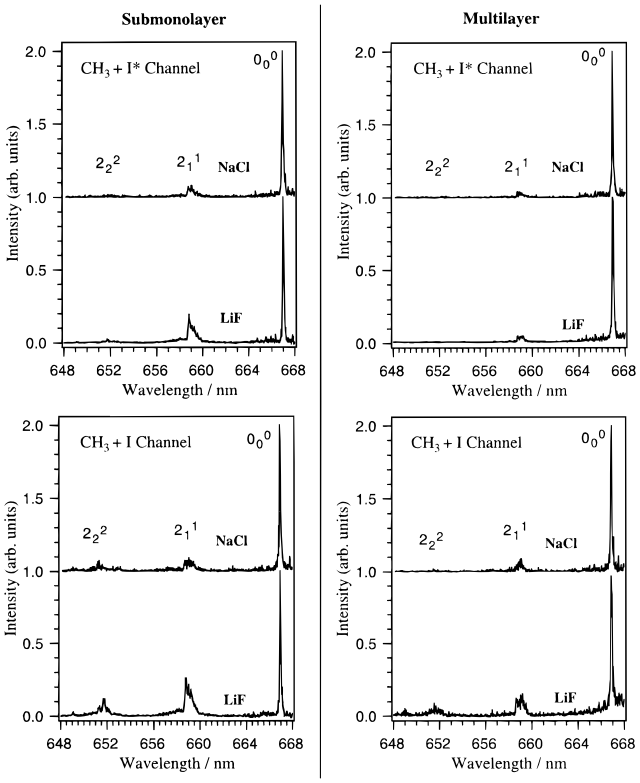

Figure 3. (2+1) REMPI spectra of the CH_3 fragments generated from photodissociation of CH_3I adsorbed on LiF(001) and NaCl(001) at submonolayer (left column) and multilayer (right column), coverages. Spectra are normalized to their peak values. Measurements were made at an angle of $\theta = 10°$ to the surface normal.

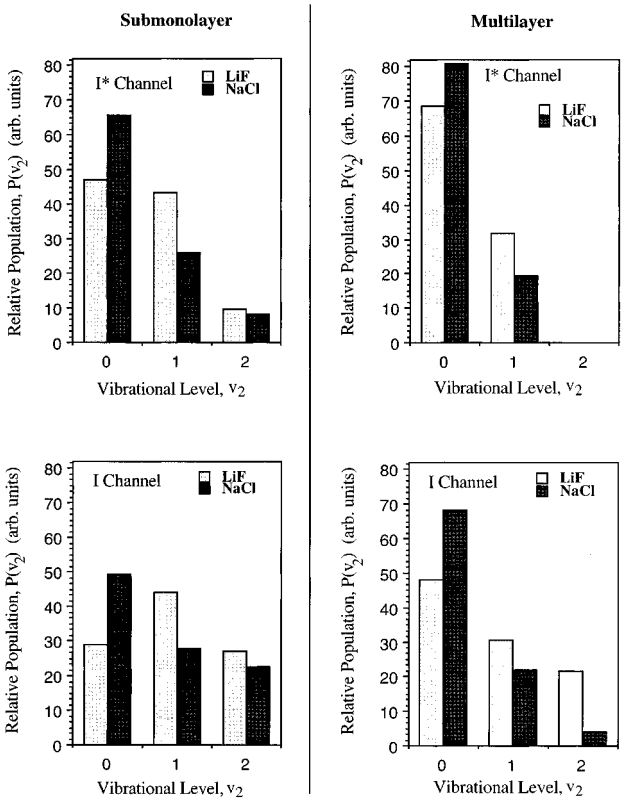

Figure 4. Vibrational state distributions of the CH_3 fragments generated from photodissociation of CH_3I adsorbed on LiF(001) and NaCl(001) at submonolayer (left column) and multilayer (right column), coverages. The total vibrational populations have been normalized to the same value.

$v_2 = 2$), the population ratio $P(v_2{=}0)/P(v_2{=}2)$ becomes 0.75 for the I channel of the CH_3I/LiF system at submonolayer coverage. The corresponding value is 1.56 for the I* channel of the same system, CH_3I/LiF. For the gas-phase the averaged ratio, $P(v_2{=}0)/P(v_2{=}2)$, for both reaction channels, I* and I, was determined to be 1.1 for photodissociation of CD_3I(g) at 266 nm and >1.1 for CH_3I(g).[10] This is similar to our measured value for CH_3I/LiF. In other gas-phase work, using the infrared diode laser techniques, the population distribution for I* channel was found for $v_2 = 0/1/2/3$ on a relative scale to be 0.66/0.26/0.08/0.004 for photodissociation of CH_3I(g) at 248 nm.[11] This is comparable to our results from photodissociation of submonolayer CH_3I/LiF at 248 nm, namely, $v_2 = 0/1/2$ being 0.47/0.43/0.1. We conclude that the vibrational population-distribution obtained from photodissociation of submonolayer CH_3I/LiF is not far removed from that observed recently by the infrared probing of CH_3 in photodissociation of gaseous CH_3I. The highly inverted vibrational populations in CH_3 suggested earlier by TOF and IR emission experiments on CH_3I(g)[5−8] were not observed here, nor in the recent definitive gas-phase experiments.[10,11]

The systematic changes of vibrational state distributions with reaction channel, surface coverage and substrate, shown in Figure 4, embody considerable information on the reaction dynamics. This will be discussed in section VI.

(C) Angular Distribution. The angular distributions of the methyl photofragments, $P(\theta)$, were recorded by monitoring the CH_3 ion-signal intensity as function of detection angle, θ, by rotating the crystal at constant angle-of-incidence of the photolysis laser. Since the crystals were mounted in such a way that the surface normal was tilted by 10° to the detection axis (see Figure 1), the minimum angle that could be measured was 10°. The angular distributions obtained are shown in Figure 5. All the angles shown in the figure have been corrected by the 10° tilt angle.[24]

For CH_3I on LiF the angular distributions exhibited a narrow peak in the region of 20−25° regardless of reaction channel or surface coverage. For CH_3I on NaCl, by contrast, a relatively broad angular distribution was obtained, peaking close to the surface normal at 0°. This was characteristic of the NaCl substrate, showing no obvious change with the surface coverage. We estimate the angular distribution on NaCl to be at least double the width of that on LiF.

For direct photodissociation by way of a repulsive excited state, as in the case of CH_3I, the angular distribution of the photofragments reflects the initial *alignment* of the adsorbates at the surfaces. Since the "direct" pathway involves the collision-free escape of CH_3(g), the *orientation* of the CH_3I-(ad) which generated this directly recoiling CH_3 is with the methyl group "up". The alignment must be with the CH_3I tilted 20−25° away from the surface normal of LiF(001). The diminished and broadened translational energy distribution for CH_3 from CH_3I/NaCl, as well as the broadened angular distribution peaking at the normal, suggests that the C−I axis is tilted further away from the surface normal than on LiF, so that the escaping CH_3 from CH_3I/NaCl collides with an adjacent CH_3I(ad). This shift in the adsorbate geometry in the direction of "lying down" could be due to the larger separation between CH_3I(ad) molecules, at all coverages, on the crystal with the larger unit-mesh size. The peak in $P(\theta)$ at $\theta = 0°$ would then be the result of widely distributed angular scattering of the CH_3. Since the loss in E_T in indirect scattering of CH_3 from CH_3I/NaCl, compared with the direct photorecoil of CH_3 from CH_3I/LiF, amounted to only a few tenths of an electronvolt, we referred to the $\vec{CH_3} + \underline{CH_3}I$(ad) collisions as weak large-impact-parameter encounters (CH_3 symbolizes nascent directly photo-

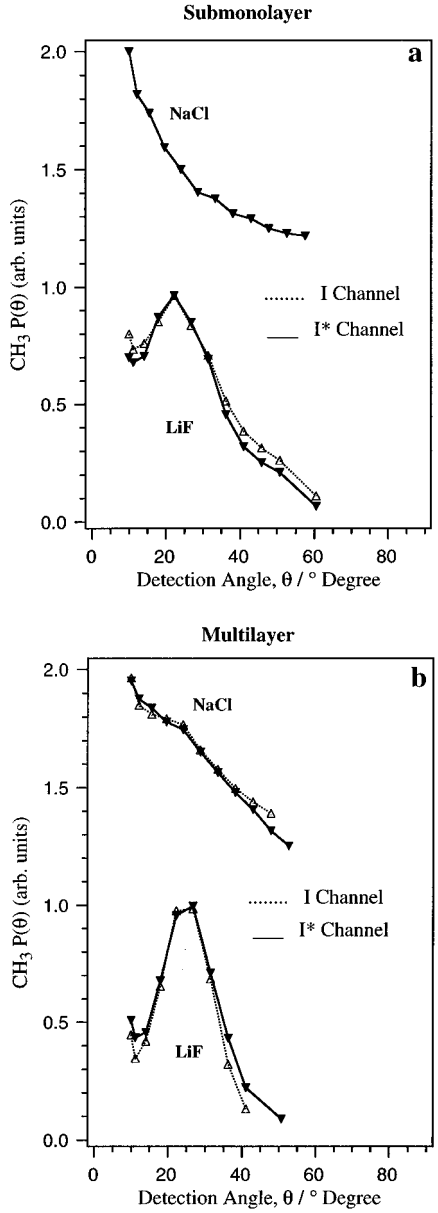

Figure 5. Angular distributions of the CH_3 fragments generated from photodissociation of CH_3I adsorbed on LiF(001) and NaCl(001) at submonolayer (left), and multilayer (right), coverages. Spectra are normalized to their peak values. Solid lines for I* channel, dashed lines for I. Measurements were for the $v_2 = 0$ vibrational state.

recoiling methyl). Such collisions would be strong enough to scatter the CH_3 widely, as observed, since a large impact-parameter encounter can cause deflection of the trajectory.

For multilayer coverages, one would expect that the structure of adsorbate tends to that for the bulk crystal. The crystal structure of CH_3I has been determined by X-ray diffraction;[26] it is isomorphous with the orthorhombic space group D_{2h}^{16}, and the unit cells contain four molecules. The C−I bond of CH_3I is aligned in the reflection plane. The CH_3I molecules in the reflection plane are oriented antiparallel to the molecules lying in the next adjacent planes. The two angles between the C−I···I are 124° and 164° (see Figure 6). The C−I bond is therefore tilted at 20° with respect to the *c* axis of the CH_3I crystal, as illustrated in Figure 6.

This tilt angle is very close to the peak position, 20−25° from surface normal, in the angular distributions we observed for CH_3I/LiF system, suggesting that the multilayer structure of CH_3I on the LiF surface has the *c* axis for the CH_3I(s) crystal

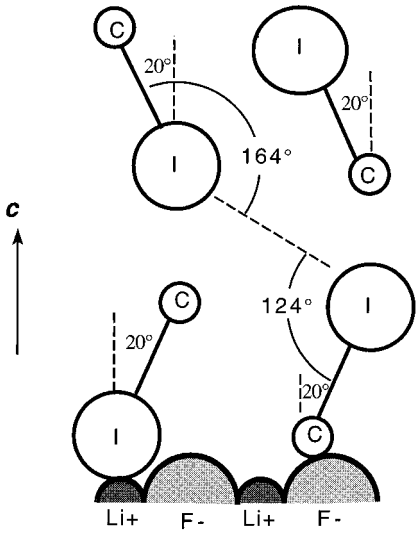

Figure 6. Schematic diagram of the geometry of CH_3I adsorbed on LiF(001) surface.

TABLE 1: I* Quantum Yield, Φ* = I*/(I* + I), in the Photodissociation of CH_3I at 248 nm

	LiF		NaCl		
vibronic band	submono-layer	multi-layer	submono-layer	multi-layer	gas phase[a]
0_0^0	0.79	0.76	0.76	0.71	0.92,[b] 0.95[c]
2_1^1	0.68	0.56	0.61	0.57	0.77[b]
2_2^2		0.34			0.50[b]

[a] Photodissociation of CH_3I at 266 nm. [b] Data from ref 10. [c] Data from ref 9a.

along the surface normal of LiF(001) (Figure 6). The antiparallel orientation of CH_3I in the crystal, with the CH_3 groups pointing alternately up and down with respect to the LiF surface, may also be evident in our experiments since a significant amount of inelastically scattered CH_3 was observed along with the direct component, particularly for multilayer coverages on NaCl.

Theory also supports the antiparallel orientation of CH_3I in the adsorbed state.[15] It is found that the CH_3I molecules are aligned perpendicular to a LiF surface with the methyl groups alternately up or down. The computed angular distribution of the CH_3 photofragments in ref 15 was found to peak at $\theta = 0°$ when CH_3 pointed up; i.e., the C−I bond axis was found to be "standing up" even at low coverage.

(D) Reaction Dynamics. Several aspects of the photodissociation dynamics of CH_3I(ad) are discussed in this section. A full analysis of the data presented above will require detailed computations on a potential-energy surface (pes) that takes account of the adsorbate−surface and adsorbate−adsorbate interactions in the two electronic states leading to I* and I products. Nevertheless there are correlations that may be illustrated by simple modeling. In particular there is the observation of reduced I* quantum yield as compared with the gas-phase, together with a systematic decrease in I*/(I* + I) as the vibrational excitation in the CH_3 product increases. A possible origin for these correlations is set out below, based on Landau−Zener surface hopping[27] and using a model on lines first proposed for the gas phase.[9c,28]

The state-resolved I* quantum yields, Φ* = I*/(I* + I), are given in Table 1 together with those from gas-phase experiments. The I* quantum yields are obtained using integrated intensities of I* and I peaks in the translational-energy distribu-

tions shown in Figure 2, and the standard deviation was <2%. They are normalized to unity for each individual case listed in Table 1.

The I* quantum yields, Φ*, for the adsorbed states of CH_3I are substantially smaller than those for the gas phase. Taking the multilayer CH_3I/LiF system as an example, Φ* decreases substantially from gas-phase values of 0.92−0.76 for 0_0^0, 0.77−0.56 for 2_1^1, and 0.50−0.34 for 2_2^2 band.

It is thought that the formation of iodine in its ground state is mainly due to curve crossing between the $^3Q_{0+}$ and $^1Q_1$ states (for details, see section I). The crossing probability between these states is described by the Landau−Zener model.[27] If the excitation is purely to the $^3Q_{0+}$ state then the I* quantum yield is[28]

$$\Phi^* = \exp\left(-\frac{2\pi V_{12}}{h|\Delta F|v}\right) \quad (1)$$

where V_{12} is the coupling term of the two states, v is the velocity at the crossing point, and ΔF is the difference in gradient of the two potential surfaces where they cross.

The value of Φ* is dependent on three variables in eq 1; V_{12}, v, and ΔF. A smaller Φ* can be the result of a larger value of V_{12} or smaller values of v and ΔF. The potential surfaces of the $^3Q_{0+}$ and $^1Q_1$ states are unlikely to be substantially modified in the physisorbed states, in view of the weak interactions. Consequently an alteration in ΔF is unlikely to be responsible for the observed decrease in I* in the adsorbed state. Neither does it seem likely that this effect is due to a change in the v term since the velocities of CH_3 fragments from adsorbed states are very similar to those from gas phase, consistent with similar velocities in the crossing region. It seems most probable that change in the V_{12} term is the most significant cause of the observed decrease in Φ*.

The V_{12} term is a measure of the coupling between the singlet $^1Q_1$ and triplet $^3Q_{0+}$ states. Enhanced coupling will result in a smaller Φ*. The dissociating CH_3I in the adsorbed state is surrounded by CH_3I molecules, especially at multilayer coverages. The strong magnetic field generated by the heavy iodine with its large atomic-number nucleus can cause enhanced coupling between the $^3Q_{0+}$ and $^1Q_1$ states. Such enhanced mixing of states due to heavy neighboring atoms, termed the "heavy-atom effect", has been observed in the liquid phase.[29] Consequently we suggest that the decrease of the I* quantum yield in the adsorbed states is due to the enhanced coupling between the two excited states caused by the "heavy-atom effect". The same explanation was also given in related work from this laboratory on the photolysis of CH_3I/Ag(111) at 248 nm.[30]

It is noteworthing that the I* quantum yield varies with the vibronic band of the CH_3 fragments; for example, for a multilayer on LiF, Φ* = 0.76, 0.56, and 0.34 for the 0_0^0, 2_1^1, and 2_2^2 bands, respectively. This variation would not be expected to be caused by the V_{12} term, since all the adsorbed CH_3I molecules are in the same environment. A more plausible source of this inverse correlation is a decrease in the velocity of approach, v, to the crossing point for trajectories that are en route to successively higher product rovibrational states. We elaborate on this below.

Energy conservation requires that highly internally excited CH_3 fragments carry less translational energy. Since the crossing point of the two excited states of CH_3I can be expected to be in the product valley of the potential-energy surface,[12] the reduced final velocity of internally excited CH_3 fragments could evidence itself in the crossing region. As a result of progressive lowering of the velocity, the I* quantum yield, Φ*, would decrease with increasing vibrational excitation in the CH_3 fragments in going from 0_0^0 to 2_2^2, as is observed to be the case.

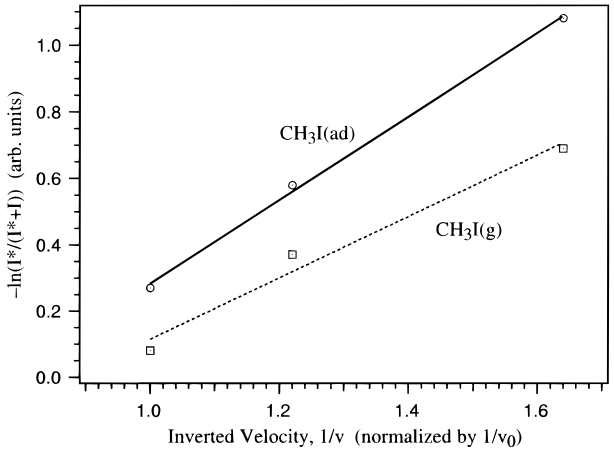

Figure 7. Landau−Zener plot. The solid line is for the CH_3I/LiF system at multilayer coverage; the dashed line is for the gas phase.[10] The solid and dashed lines are linear least-squares fits to the data points. The quantity $(1/v)$ has been normalized by division by $(1/v_0)$, where v_0 is the calculated velocity at the p.e. curve-crossing point for CH_3 in its ground state, $v_2 = 0$.

The Landau−Zener plot is shown in Figure 7 using both the Φ* obtained in this work and that for the gas-phase experiments, and the velocities at the crossing point calculated assuming that the fraction (though not the amount) lost to internal energy is the same at the crossing point as in final products. The linearity of the plot in Figure 7, based on eq 1, indicates that the alteration in velocity at the crossing point could be responsible for the observed decrease in I* quantum yield with increasing vibrational excitation of the CH_3 fragments.

The same model has been used to discuss the photolysis of CD_3I(g) at 266 nm. A correlation between the velocity of CD_3 fragments at curve crossing and the observed I* quantum yield was obtained.[9c] This "velocity factor" was invoked as well in the gas-phase photodissociation of CH_3I, C_2H_5I, *n*-C_3H_7I, and *n*-C_4H_9I.[28] In this case, the decrease of Φ* was attributed to a possible decrease of the velocity in the crossing region as the dissociating molecules increased in complexity.

The dependence of vibrational state distribution in CH_3 on reaction channel, coverage, and substrate will be discussed next.

The CH_3 fragments were found to be less vibrationally excited in the I* channel than in the I channel, in the photodissociation of adsorbed CH_3I for a given substrate and coverage (compare top and bottom panels in Figure 4). Similar results were also obtained in gas-phase experiments.[9−11] The reason is thought to be the difference in the pes corresponding to the two reaction channels. The pes of the $^3Q_0$ state, which leads to I* + CH_3, involves a smaller repulsive energy release (by 0.94 eV) than that of the $^1Q_1$ state which generates I + CH_3.[12] As a result the CH_3I molecules dissociating on the $^3Q_0$ surface are subject to a smaller impulse than those on the $^1Q_1$ surface, resulting in less vibrational excitation of the CH_3 fragments in the I* channel. This is in accord with the results from the theoretical study of the CH_3I/LiF system, which also showed higher vibrational excitation of CH_3 fragments in the I channel.[15]

As discussed in section III.B, the vibrational-state distribution for the I channel of the submonolayer CH_3I/LiF system was similar to that for the gas phase. However, for all other cases, i.e., altered substrate or coverage, the vibrational excitations tended to be cooler, indicative of vibrational deexcitation of CH_3. Furthermore, the vibrational excitation of the CH_3 photofragments was less for multilayer than for submonolayer

coverage for a given reaction channel and substrate, and it was less for the NaCl substrate than for LiF (for a given reaction channel and coverage). The variation of vibrational-state distribution with coverage and substrate is likely to be linked to changing geometry of the adlayer, which affects the probability that photorecoiling $\vec{CH_3}$ suffers an inelastic collision. The deexcitation of the $\vec{CH_3}$ vibrations can result from inelastic collisions between $\vec{CH_3}$ and the substrate, or (more efficiently) between $\vec{CH_3}$ and adjacent CH_3I(ad). These deexcitation pathways were evident in the theoretical study of the CH_3I/LiF system.[15]

Comparison of the translational-energy distribution curves in Figure 2 for CH_3 from CH_3I/LiF (solid lines) with those from CH_3I/NaCl (broken lines) shows that there is invariably a lower peak translation for CH_3I/NaCl than for CH_3I/LiF. Since this decrease in peak translational energy is observed at both submonolayer and multilayer coverage, it cannot be due to increased energy transfer to the NaCl substrate. Instead it is likely to be due to altered energy transfer in collisions between $\vec{CH_3}$ and CH_3I(ad). A change in the geometry of the adlayer with substitution of NaCl for LiF would alter, for example, the mean impact parameter in a $\vec{CH_3}$ + CH_3I(ad) encounter. A similar effect is found in the angular scattering of methyl (Figure 5), which is broader on NaCl than on LiF. Lower impact parameter $\vec{CH_3}$ + CH_3I(ad) collisions on the NaCl substrate, as compared to LiF, would give rise to greater energy transfer and wider angular scattering, as observed. A tilt of the C−I axis for CH_3I on NaCl further away from the normal than the 20−25° applicable to the case of LiF, would account for the stronger $\vec{CH_3}$ + CH_3I(ad) encounters in the NaCl case. A more-nearly "lying down" configuration on NaCl is plausible in light of the larger ionic mesh for NaCl.[24]

An alternative source of the decreased peak translational energy on NaCl, which we cannot at present entirely discount, would be a stronger bonding of CH_3 to neighboring CH_3I(ad) on the NaCl crystal. This would diminish the translational energy available to the CH_3(g). However, stronger binding of CH_3 in CH_3I(ad) to neighboring absorbed molecules at multilayer coverages on NaCl compared with submonolayer should then further decrease the translational energy of CH_3(g), but this is not observed. A further weakness in this scenario is that bonding of the CH_3 group to adjacent adsorbate molecules would tend to tether the H atoms, resulting in enhanced inversion vibrational excitation following the photorecoil of the carbon atom in H_3C away from its adjacent I as H_3C·I dissociates. No such enhancement in $P(v_2=2)/P(v_2=0)$ is observed in going from LiF to NaCl (see Figures 3 and 4).

On balance it appears more likely that there is a tilting of the CH_3I further from the normal on NaCl than on LiF, as postulated above. Polarized FTIR or similar studies are needed, however, to establish conclusively the source of the decreased translational and vibrational deexcitation, as well as the broadened angular distribution for CH_3 photorecoiling from CH_3I/NaCl rather than from CH_3I/LiF.

IV. Summary and Conclusions

The photodissociation of CH_3I on LiF(001) and NaCl(001) at 248 nm has been studied by probing the CH_3 fragments using resonantly enhanced multiphoton ionization and time-of-flight mass spectrometry. The translational energy, vibrational state and angular distributions of the CH_3 photofragments were determined for both the CH_3I/LiF and the CH_3I/NaCl systems, at submonolayer and multilayer coverages. The major experimental findings are given below. This is followed by a summary of the dynamical implications.

(1) For the particular case of adsorbate photolysis in CH_3I/LiF two translational-energy peaks in the photorecoiling CH_3, relating to the I* and I channels, approximated in energy the corresponding peaks observed in the gas phase. For CH_3I/NaCl these peaks were broader and shifted to lower translational energy as compared to CH_3I/LiF.

(2) The vibrational-state distributions in CH_3 obtained from the photodissociation of submonolayer CH_3I/LiF also resembled those in photodissociation of gaseous CH_3I. However, the vibrational excitation was diminished for the NaCl substrate, and for multilayer coverages on both substrates.

(3) The angular distribution showed a narrow peak at approximately 20° with respect to the surface normal for the case of CH_3I/LiF. By contrast for CH_3I/NaCl a broad angular distribution peaking at 0° was obtained.

(4) The $\Phi^* = I^*/(I^* + I)$ quantum yields from three vibrational states of adsorbed CH_3I were substantially smaller than those in the gas phase. The magnitude of Φ^* decreased with increasing vibrational excitation of the CH_3 photofragment.

The photodissociation dynamics of CH_3I(ad) has been discussed in the following terms. A deexcitation mechanism involving directed photorecoiling $\vec{CH_3}$ in collision with adjacent CH_3I(ad) was proposed to account for the increased loss of translational energy, loss of vibrational excitation, and the broadening of the angular distribution, all of which were observed on the NaCl substrate. The enhanced inelastic collision probability in the case of CH_3I/NaCl suggested a more-nearly "lying down" geometry of CH_3I on NaCl as compared with the "standing up" one on LiF (20° from the normal). The larger ionic mesh size for NaCl could account for an increased tendency for CH_3I to lie down on this substrate.

Enhanced coupling between the two excited states, $^1Q_1$ and $^3Q_0$, caused by the "heavy-atom effect" is thought to be responsible for the substantially decrease in Φ^* for CH_3I(ad) compared with for CH_3I(g). The observed substantial decrease in Φ^* with vibrational excitation was attributed to diminishing velocity, v, at the crossing point between the two excited states. Using the Landau−Zener approximation a linear relation was obtained between $\ln \Phi^*$ and $1/v$, in accordance with this model.

Acknowledgment. The authors wish to acknowledge generous assistance from the Natural Sciences and Engineering Research Council of Canada (NSERC), the Ontario Laser and Lightwave Research Centre (OLLRC), and the New Energy and Industrial Technology Development Organization (NEDO) of Japan. N.S.-K.S. is grateful to the Croucher Foundation for the award of a postdoctoral fellowship.

References and Notes

(1) For recent reviews on surface photochemistry see: (a) Ho, W. *Surf. Sci.* **1994**, *299/300*, 996. (b) Zhu, X.-Y. *Annu. Rev. Phys. Chem.* **1994**, *45*, 113. (c) Polanyi, J. C.; Zeiri, Y. In *Laser Spectroscopy and Photochemistry on Metal Surfaces*; Dai, H.-L., Ho, W., Eds.; World Scientific: River Edge, NJ, 1995; Vol. II, p 1241.

(2) (a) Polanyi, J. C.; Williams, R. J. *J. Chem. Phys.* **1988**, *88*, 3363. (b) Polanyi, J. C.; Rieley, H. In *Dynamics of Gas-Surface Interactions*; Rettner, C. T., Ashfold, M. N. R., Eds.; Royal Society of Chemistry: London, 1991; p 329.

(3) Lee, Y. T. *Angew. Chem., Int. Ed. Engl.* **1987**, *26*, 939.

(4) Lin, M. C.; Sanders, W. A. In *Advances in Multi-Photon Processes and Spectroscopy*; Lin, S. H., Ed.; World Scientific: River Edge, NJ, 1986; p 333.

(5) Sparks, R. K.; Shobatake, K.; Carlson, L. R.; Lee, Y. T. *J. Chem. Phys.* **1981**, *75*, 3838.

(6) van Veen, G. N. A.; Baller, T.; de Vries, A. E.; van Veen, N. J. A. *Chem. Phys.* **1984**, *87*, 405.

(7) Barry, M. D.; Gorry, P. A. *Mol. Phys.* **1984**, *52*, 461.

(8) (a) Baugheum, S. L.; Leone, S. R. *J. Chem. Phys*. **1980**, *72*, 6531. (b) Pence, W. H.; Baugheum, S. L.; Leone, S. R. *J. Phys. Chem*. **1981**, *85*, 3844. (c) Hermann, H. W.; Leone, S. R. *J. Chem. Phys*. **1982**, *76*, 4759; 4766.

(9) (a) Chandler, D. W.; Houston, P. L. *J. Chem. Phys*. **1987**, *87*, 1445. (b) Chandler, D. W.; Thoman, J. W., Jr. *Chem. Phys. Lett*. **1989**, *156*, 151. (c) Chandler, D. W.; Janssen, M. H.; Stolte S.; Strickland, R. N.; Thoman, Jr, J. W.; Parker, D. H. *J. Phys. Chem*. **1990**, *94*, 4839.

(10) Ogorzalek Loo, R.; Hueri, H.-P.; Hall, G. E.; Houston, P. L. *J. Chem. Phys.* **1989**, *90*, 4222.

(11) Suzuki, T.; Kanamori, H.; Hirota, E. *J. Chem. Phys*. **1991**, *94*, 6607.

(12) For references see: Yabushia, S.; Morokuma, K. *Chem. Phys. Lett*. **1988**, *153*, 517 and references within.

(13) Kutzer, J.; Lindeke, G.; Welge, K. H.; Feldman, D. *J. Chem. Phys*. **1989**, *90*, 548.

(14) (a) Fairbrother, D. H.; Trentelman, K. A.; Strupp, P. G.; Stair, P. C.; Weitz, E. *J. Vac. Sci. Technol. A* **1992**, *10*, 2243. (b) Trentelman, K. A.; Fairbrother, D. H.; Strupp, P. G.; Stair, P. C.; Weitz, E. *J. Chem. Phys*. **1992**, *96*, 9221. (c) Fairbrother, D. H.; Briggman, K. A.; Stair, P. C.; Weitz, E. *J. Chem. Phys.* **1995**, *102*, 7267.

(15) Huang, Z.-H.; Guo, H. *J. Chem. Phys*. **1993**, *98*, 3395.

(16) Jackson, R. C.; Polanyi, J. C.; Sjövall, P. *J. Chem. Phys.* **1995**, *102*, 6308.

(17) Polanyi, J. C.; Sze, N. S−K.; Wang, J.-X., in preparation.

(18) Chemie, V. F. Ph.D. Dissertation; University of Hannover: Hannover, Germany, 1992; p 54.

(19) Heidberg, J.; Kampshoff, E.; Schönekäs, O.; Stein, H.; Weiss, H. *Ber. Bunsen-Ges. Phys. Chem*. **1990**, *94*, 112.

(20) Lee, T. G.; Liu, W.; Polanyi, J. C., to be published.

(21) Calculated using the dissociation energy of CH_3I, ∼2.3 eV, reported in refs 6 and 7.

(22) Okabe, H. *Photochemistry of Small Molecules*; Wiley-Interscience: New York, 1978; p 372.

(23) Giorgi, J. B.; Kühnemuth, R.; Polanyi, J. C.; Wang, J.-X. *J. Chem. Phys.* **1997**, *106*, 3129.

(24) (a) Garrett, S. J.; Heyd, D. V.; Polanyi, J. C. *J. Chem. Phys.* **1997**, *106*, 7834. (b) *Ibid.* **1997**, *106*, 7847.

(25) (a) Black, J. F.; Powis, I. *J. Chem. Phys.* **1988**, *89*, 3986. (b) Black, J. F.; Powis, I. *Chem. Phys.* **1988**, *125*, 375.

(26) Kawaguchi, T.; Hijikigawa, M.; Hayafuji, Y.; Ikeda, M.; Fukushima, R.; Tomiie, Y. *Bull. Chem. Soc. Jpn.* **1973**, *46*, 53.

(27) (a) Landau, L. D. *Phys. Z. Sowj. Un*. **1932**, *2*, 46. (b) Zener, C. *Proc. R. Soc. A* **1932**, *137*, 696.

(28) Godwin, F. G.; Paterson, C.; Gorry, P. *Mol. Phys*. **1987**, *61*, 827.

(29) McGlynn, S. P.; Smith, F. J.; Cilento, G. *Photochem. Photobiol*. **1964**, *3*, 269.

(30) Jensen, E. T.; Polanyi, J. C. *J. Phys. Chem*. **1993**, *97*, 2257.